CHRONOLOGY OF THE BAXIE LOESS PROFILE AND THE HISTORY OF MONSOON CLIMATES IN CHINA BETWEEN 17,000 AND 6000 YEARS BP

WEIJIAN ZHOU, ZHISHENG AN, BENHAI LIN, JULE XIAO, JINZHAO ZHANG
JUN XIE, MINGFU ZHOU

Xi'an Laboratory of Loess and Quaternary Geology, Academia Sinica, Xi'an 710061
Shaanxi Province, Peoples Republic of China

S. C. PORTER[1], M. J. HEAD[2] and D. J. DONAHUE[3]

ABSTRACT. The valley of the Baxie River, situated in the western region of the Loess Plateau in central China, contains a loess profile 15 m thick, which can be considered representative of loess-paleosol sequences formed over the last 17 ka. Both thermoluminescence (TL) determinations on fine-grained sediment (4–11 μm) and ^{14}C determinations on various organic fractions of paleosols from the profile have provided an extremely useful chronological framework for these sequences. These sequences indicate a weakened summer monsoon during the last glacial maximum followed by a strengthening of the summer monsoon, beginning *ca.* 13 ka cal BP. An abrupt change to a weakened summer monsoon regime lasted from *ca.* 10.9 to 10.2 ka cal BP. The Asian summer monsoon circulation, recording the Holocene optimum, then increased and lasted from *ca.* 10.2 to 6 ka cal BP. The organic component of samples taken down the profile has δ^{13}C values ranging from −21 to −24‰ with respect to the PDB standard. The more positive δ^{13}C values suggest that the proportion of C_4-type plants in river valleys of the Loess Plateau increased as Asian summer monsoon influence weakened, and C_3-type vegetation increased as the summer monsoon influence strengthened. Magnetic susceptibility and organic content were low during loess deposition, also reflecting weakening of summer monsoon. Two ^{14}C determinations on the humin fraction of the organic component near the top of the lower paleosol and the base of the upper paleosol complex gave ages of 10.2 and 10.9 ka cal BP, respectively. These ages mark the beginning and termination of a brief event involving increased dust influx under weakened summer monsoon conditions.

INTRODUCTION

The Loess Plateau of China is located in the mid-latitudes of the northern hemisphere, averaging 1000–1500 m above sea level (Fig. 1). The area is influenced by the southeast and southwest monsoon system. Loess-paleosol sequences were formed over the last 2.5 Ma (Liu 1985; Heller & Liu 1986). The paleomonsoon records in the loess-paleosol sequences of the past 2.5 Ma and 130 ka have been reported, respectively, by An *et al.* (1991, 1990). We consider here the period since 17 ka BP.

Distinct wet and dry seasons characterize the Loess Plateau at present. The loess is deposited with the cold and dry winter monsoon circulation, and the paleosol forms when the wet summer monsoon is dominant. Two major factors cause such an obvious monsoon effect. First is the pressure gradient between the continent and the Pacific and Indian Oceans due to their differing heat capacities and expected differential response to solar radiation. Because the heat capacity of the ocean is much larger than that of the land surface, the land becomes warmer than the ocean in summer, forming a low-pressure system above the land surface and a high-pressure system above the sea surface. This phenomenon reverses during winter. Second, the still-uplifting Qinhai-Xizhang Plateau strongly influences monsoon variations. In winter, the plateau surface loses heat rapidly and is colder than the surrounding atmosphere, forming a cold high-pressure system that overlaps the Mongolian high-pressure system, strengthening the winter monsoon. In summer, a hot, low-

[1]Quaternary Research Center, University of Washington, Seattle, Washington 98195 USA
[2]Radiocarbon Dating Research Unit, Research School of Pacific Studies, Australian National University, Canberra, ACT 2601 Australia
[3]NSF-Arizona Accelerator Facility for Radioisotope Analysis, The University of Arizona, Tucson, Arizona 85721 USA
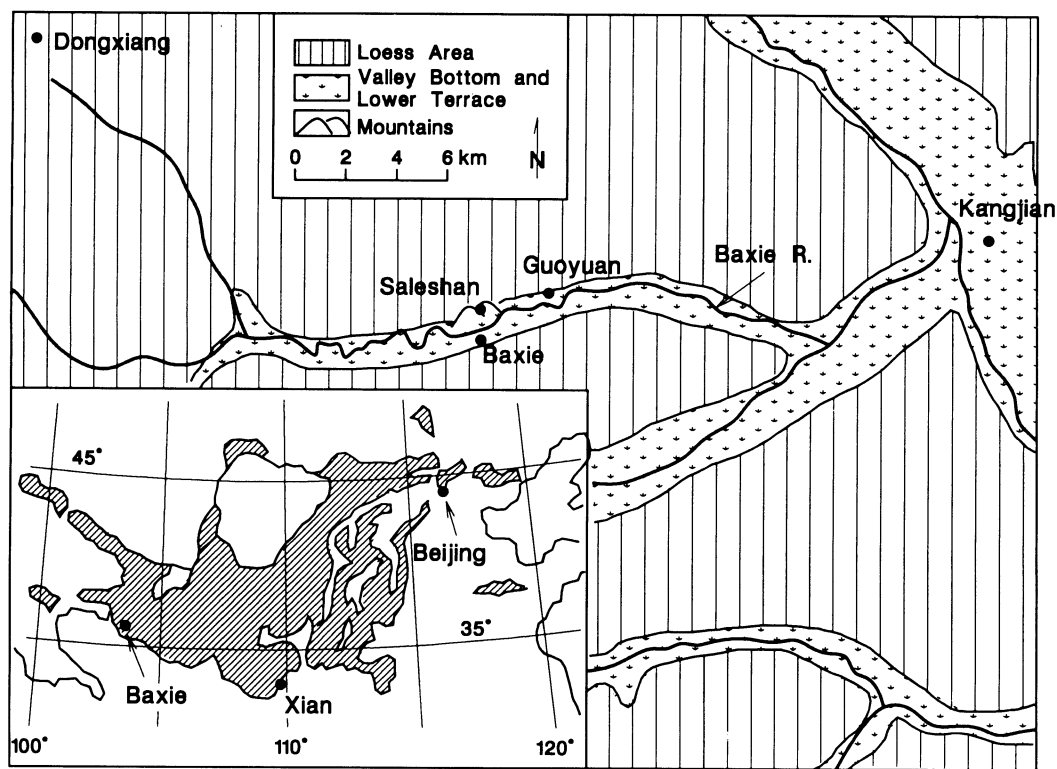
Fig. 1. Map showing location of Baxie loess profile

pressure system above the plateau surface overlaps and strengthens the Indian continental low-pressure system, strongly drawing monsoon air farther inland.

Thus, summer climate in China is controlled by the continental Indian thermal low-pressure and the subtropic high-pressure systems. The inflow of warm and humid air from the ocean to land brings precipitation. In winter, the main influences are the Mongolian high-pressure system and the Aleutian and equatorial low-pressure system. A cold and dry northwest wind prevails on the Loess Plateau, and is the major mechanism for dust transportation. The continuous loess-paleosol sequences record the magnitude of the winter and summer monsoons in China. Accurate dating of loess and paleosols, combined with other climatic proxy indexes, enables us to reconstruct the history of paleomonsoon changes within the Loess Plateau over the last 17 ka.

An initial ^{14}C chronological framework for the Loess Plateau in China was established in the mid-1980s (Zheng 1985; Qiao 1985). Many ^{14}C results indicate possible younger contamination, leading researchers to consider the ages as minimum only. Head, Zhou and Zhou (1989) and Zhou, Zhou and Head (1990) studied one section in the Loess Plateau (Bei Zhuang Cun) in great detail, and established a reliable chronology after developing specific sample pretreatment techniques for the site.

We chose the Baxie Loess Profile in Gansu Province (Fig. 1) for further chronological studies because of the relatively rapid sediment accumulation rate and, hence, good stratigraphic resolution. Zhang (1989) previously studied this profile to ascertain the frequency of landslides in the area. We collected a series of loess and paleosol samples and separated different organic and inorganic

fractions for dating, using liquid scintillation and AMS techniques, then compared the results with those obtained from eolian dust, using the TL technique. This provided a cross-check to ensure a reliable chronology for terrestrial sediments, so that correlations could be made among sea, land and atmospheric data. We also used $\delta^{13}C$, magnetic susceptibility (SUS) and total organic carbon content (TOCC) measurements to define the sedimentary sequences indicating environmental change.

Measured SUS is the induced magnetization of objects in an artificial weak magnetic field. The principle carrier in loess and paleosol sediments is ultrafine (<1 μm) magnetite and maghemite (Kukla & An 1989). The ultrafine single-domain grains display superparamagnetism, and provide the main contribution to the SUS signal. These minerals may arrive as a component of eolian dust from source areas. Alternatively, they may originate through pedogenic processes (Maher & Thompson 1992). Because dust accumulation and pedogenesis are interconnected processes, SUS represents a potential proxy index of climate variability closely related to past changes of precipitation caused by monsoon variations. When the summer monsoon dominated, precipitation increased and the climate was warm, resulting in the paleosol section of the profile, with a denser plant cover providing high SUS, high TOCC and more negative $\delta^{13}C$ values. Thus, SUS, TOCC and $\delta^{13}C$ values are sensitive proxy indexes for summer and winter monsoon intensity.

We consider here the period from 17 to 6 ka BP in the history of monsoon climates in China as recorded in the Baxie River valley of the Loess Plateau of China. The Baxie profile is sensitive to monsoon variation and records the history of paleomonsoon changes within this range, showing not only climatic reversals, but also the Holocene optimum.

GEOLOGICAL AND CLIMATIC SETTING OF THE BAXIE SECTION

The Baxie profile (Fig. 1) is in Gansu Province on the second terrace of the Baxie River (103° 35′E, 35°34′N) at the southwestern edge of the Loess Plateau, to the south of Sale Mountain, 65 km southwest of Lanzhou. Since the Pliocene, the area (elevation *ca.* 2000 m) has suffered large-scale neotectonic uplift. More than 100 m of loess overlie a basal layer of red, compacted silty clay of upper Pliocene age, which is common throughout the Loess Plateau (Liu 1985). The Baxie River is a third-order tributary of the Yellow River, which, along with its many tributaries, has cut down through this section.

The Baxie profile is in a temperate, semi-arid steppe climatic zone with distinct wet and dry seasons. June–September rainfall is about 72% of total annual precipitation. Thick layers of loess accumulate under the steppe-desert landscape during cold and dry climatic sequences. Paleosols formed under steppe-forest conditions during warm and humid climatic periods. Total annual evaporation (1372 mm) exceeds precipitation (449 mm) by a factor of *ca.* 3, and the annual mean temperature is 6.3°C (Guang He Meteorological Station 1971–84; Zhang 1989).

The Baxie profile (Fig. 2) is 15 m thick, and consists of yellowish-gray loess (15.00–10.00 m depth), a weakly developed light grayish-brown paleosol (10.00–9.25 m), coarse-grained loess (9.25–8.00 m), a dark grayish-brown/black loam-type paleosol complex with a high carbonate content (8.00–4.90 m), and, above 4.90 m, reworked loess.

THE DATING EXPERIMENT

We collected three samples for TL dating and four paleosol samples for ^{14}C dating (Fig. 2). For ^{14}C dating, we collected samples of black loam paleosol with a high carbonate content. Paleosol
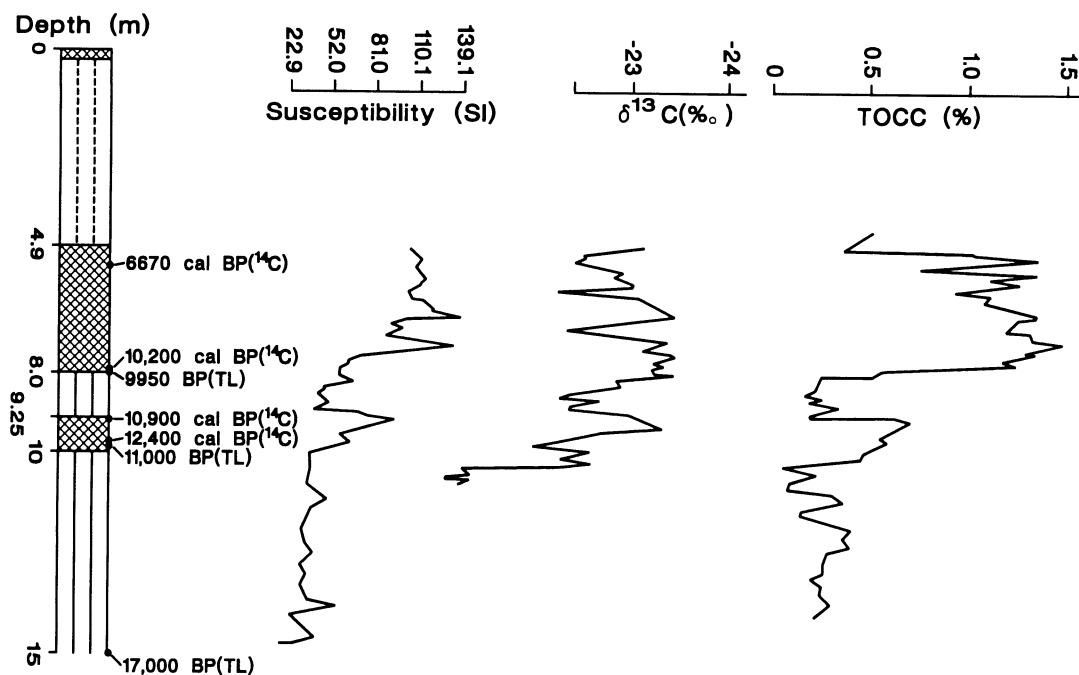
Fig. 2. Plot *vs.* depth in the Baxie profile of various measured quantities. Calendar ages *vs.* depth in the profile as deduced from ^{14}C and TL dating are also shown.

organic carbon is mainly derived from degraded plants and animal residues. Mineral carbon comes from dissolved and reprecipitated secondary carbonate.

In general, stable organic matter (humus) comprises 1/3 unhumified substances (carbohydrates, lipids, fatty acids, fats, waxes and resins) and 2/3 humified remains of plant and animal tissues (Stevenson 1986). To obtain a reliable fraction for dating, we first removed carbonate by acid treatment, then carried out successive solvent extractions, using chloroform/ethanol (2:1), ethanol and distilled water to remove any mobile organic components. We then separated humus from humin by successive leaches with 5% NaOH, and dated both of these fractions (Head, Zhou & Zhou 1989). Since the sediments in the sequence have pH ranges between 8 and 9, the paleosol layers contain a relatively high proportion of carbonate, because evaporation exceeds precipitation in the area.

To test the hypothesis that a component of this carbonate represents the period of paleosol pedogenesis, we chose paleosol sample XLLQ 442, and chemically separated primary and secondary carbonates by successive CO_2 evolution, using 50% acetic acid and 10% HCl solutions, respectively. Both were dated and compared with humus and humin fractions in the same layer (Table 1). We synthesized benzene from the various fractions for liquid scintillation spectrometry, using a Wallac Quantulus spectrometer, and we prepared graphite for AMS (Slota *et al.* 1987). Radiocarbon ages less than 8000 BP were converted to calendar ages according to the calibration curves of Stuiver and Pearson (1986). Ages greater than 8000 BP were converted to calendar ages, using the calibration table in Stuiver *et al.* (1991).

We first removed the surface of TL samples under red light, took 50 g for H_2O measurement, and subjected 100 g to further pretreatment – H_2O_2 to remove organics, 50% HCl to remove carbonate,

TABLE 1. Radiocarbon Results for Paleosols from the Baxie Profile

Sample no.	Lab no.	Depth (m)	Dating material	$\delta^{13}C$ (‰)	^{14}C age (BP)
BX8807	XLLQ442*	5.25	Sec $CO_3^=$	−5.40 ± 0.20	5900 ± 100
BX8807	XLLQ442*	5.25	Humin	−23.64 ± 0.20	5800 ± 220
BX8807	XLLQ442*	5.25	Humus	−24.68 ± 0.20	4600 ± 100
BX8807	XLLQ442*	5.25	TOC	−24.00 ± 2.0[†]	5400 ± 100
BX8806	XLLQ416*	7.75	Humin	−24.23 ± 0.20	9330 ± 220
BX9906	XLLQ416*	7.75	Humus(1)	−24.66 ± 0.20	8200 ± 160
BX8806	AA6443**	7.75	Humus(2)	−25.00 ± 0.20	8020 ± 80
BX8806	AA6444**	7.75	Humus(3)	−25.00 ± 0.20	7700 ± 70
BX8804	XLLQ415*	9.25	Humin	−23.97 ± 0.20	9830 ± 270
BX8804	XLLQ415*	9.25	Humus(1)	−25.79 ± 0.20	9310 ± 180
BX8804	AA6441*	9.25	Humus(2)	−25.00 ± 0.20	9580 ± 85
BX8804	AA6442**	9.25	Humus(3)	−25.00 ± 0.20	9695 ± 95
BX8804	XLLQ415*	9.25	TOC	−24.00 ± 0.20	8220 ± 130
BX8803	XLLQ441*	9.75	Humin	−25.02 ± 0.20	11,110 ± 220

*Xi'an Laboratory for Loess and Quaternary Geology
**NSF-Arizona AMS Facility
[†]$\delta^{13}C$ error = 2.0 indicates value is estimated

and the 4–11 μm grain-size fraction isolated by repeated Stokes settling for measuring equivalent dose for dating. We used partial bleaching (Wintle & Huntley 1982), residual TL (Singhvi, Sharma & Agrawal 1982) and regeneration TL (Readhead 1982) methods for paleodose measurement. We calculated the annual dose rate received by the sample using the relationship proposed by Aitken (1985), which includes terms for contributions from environmental U, Th and K_2O. We measured U and The contents by neutron activation analysis and K_2O by atomic absorption spectrometry. We estimated the small dose rate contributed by cosmic radiation from the burial depth, altitude and latitude of the sample (Prescott & Stephan 1982), and made a correction for H_2O content using the method of Fleming (1979).

THE MAGNETIC SUSCEPTIBILITY RECORD

SUS signals from the loess-paleosol sequence come from <1 μm grain-size material composed mainly of magnetite and maghemite (Kukla & An 1989). If we assume a constant deposition rate of this fine material, we would expect no variation in magmetic susceptibility with depth. The experimental data, however, show a higher susceptibility in paleosol samples, which indicates a higher concentration of fine-grained material. Maher and Thompson (1992) showed that pedogenesis is the cause of this phenomenon. High susceptibility indicates slow deposition rate of dust and strong pedogenesis, whereas low susceptibility reflects a rapid deposition rate of dust and weak pedogenesis. Studies of humic substances in lake water and lake sediments provide evidence that adsorbed humic substances enhance the colloidal stability of haematite particles, since the adsorbed layer prevents aggregation (Steinberg & Muenster 1985). Hence, humic substances adsorbed in paleosol clays may provide the stabilizing influence for the fine grains of magnetite. Figure 2 includes a plot of susceptibility index *vs.* depth. The pale yellowish loess (15.00–10.00 m depth) provided a minimum susceptibility index of *ca.* 34 for the profile. From *ca.* 13–10.87 ka cal BP, at a depth of 10.00–9.25 m, the SUS index increased to 95, producing two peaks, corresponding to a weak paleosol layer. From 9.25–8.00 m, the susceptibility index showed an abrupt drop to *ca.*

43, lasting for *ca.* 700 yr. The sediment from 8.00–4.90 m is a paleosol complex with two distinct peaks in susceptibility, suggesting two paleosol layers. We did not analyze the reworked loess above 4.90 m.

We conclude that as the summer monsoon strengthened, precipitation increased, leading to dense vegetation and enhanced pedogenesis. The increased proportion of the fine-grained magnetite fraction is reflected by a higher susceptibility value. As the summer monsoon weakened, the winter monsoon became dominant and precipitation decreased, making vegetation scarce. The proportion of coarse-grained material in the accumulated dust increased, as shown by the lower susceptibility values.

STABLE CARBON ISOTOPE AND TOTAL ORGANIC CARBON CONTENT

We divided into two groups samples collected at intervals of 10 cm. We made $\delta^{13}C$ determinations for one group of samples, using a Finnigan MAT 251 mass spectrometer, and measured TOCC for the other group. Both $\delta^{13}C$ and TOCC curves in Figure 2 show peaks at 10.00–9.25 m, $\delta^{13}C$ being more negative, whereas TOCC is high, the interval corresponding to the immature paleosol. A trough at 9.25–8.00 m corresponds to a thick accumulation of loess, $\delta^{13}C$ being more positive and the TOCC being low. A wide peak above 8.0–4.9 m occurs for both $\delta^{13}C$ and TOCC, corresponding to the paleosol complex. The $\delta^{13}C$ values of the whole profile range from −21 to −24‰. The somewhat more positive $\delta^{13}C$ values reflect an increased C_4 grass-to-shrub ratio and imply increased aridity. Conversely, when the summer monsoon dominated, $\delta^{13}C$ was more negative, and the proportion of C_3 plants was higher. The narrow $\delta^{13}C$ range of ~3‰ suggests a mixed flora of C_3 and C_4 plants in the Baxie River Valley, that does not change much in relative proportions. TOCC is less than 2%, both for loess and paleosol samples; the lowest values are in loess samples. The peaks and troughs of the TOCC curve are generally similar to those for SUS and $\delta^{13}C$. Thus, TOCC likely reflects not only monsoon variations, but also the density of vegetation cover (*i.e.*, changes of biomass).

RESULTS AND DISCUSSION

In Table 1, we list the results of radiocarbon measurements for several different chemical fractions from organic material obtained from the Baxie profile. Previous measurements of paleosol samples indicate that the humin fractions give most reliable ages. Calibrated ages for humin fractions are given in Table 2 and shown in Figure 2.

TABLE 2. Calibrated Ages of Humin Samples

Sample no.	Depth (m)	^{14}C age (yr BP)	Calibrated age (yr BP)
BX8007	5.25	5800 ± 200	1σ: 6940–6400*
			2σ: 7230–6230
BX8006	7.75	9330 ± 220	10,200**
BX8004	9.25	9830 ± 270	10,870**
BX8003	9.75	11,110 ± 220	12,400**

*From Stuiver and Pearson (1986)
**From Stuiver *et al.* (1991: Table 1). No estimate of the uncertainty of these calendar ages was attempted, but we expect that the 2σ range of calibrated ages would extend over about 1 ka, as it does for Sample BX8007.

TABLE 3. TL Results for Loess and Paleosol from the Baxie Profile

Sample no.	Depth (m)	U (ppm)	Th (ppm)	K (%)	H₂O (%)	ED(Gy)	Activity	Gy/ka	TL ka BP
BX-8805	7.9	2.28	10.3	2.08	3.0	41.2 ± 3.4	0.054 ± 0.001	4.09	9.95 ± 0.58
BX-8802	9.8	3.97	10.9	2.52	6.3	55.3 ± 3.3	0.048 ± 0.004	5.02	11.00 ± 0.82
BX-8801	15	2.76	10.4	1.85	4.0	69.3 ± 4.4	0.056 ± 0.002	4.06	17.2 ± 0.89

As mentioned earlier, evaporation significantly exceeds precipitation in this area, so the leaching depth of carbonate would be expected to be limited. The secondary carbonate fraction for ^{14}C sample XLLQ442 is not significantly different in age from the humin fraction, suggesting that the carbonate formed during pedogenesis and truly represents the age of paleosol development.

TL ages obtained for one loess and two paleosol samples are given in Table 3. The two TL/^{14}C pairs BX-8802/BX-8803 and BX-8805/BX-8806 were chosen because the TL and ^{14}C samples were adjacent to each other within the profile. In both cases, the TL and calibrated ^{14}C dates are not significantly different, but both sets of measurements have large errors.

INTERPRETATION OF PALEOMONSOON VARIATIONS

The curves of magnetic susceptibility, $\delta^{13}C$ and TOCC from the Baxie profile clearly reflect the history of paleomonsoon strengthening and weakening between 17 and 6 ka cal BP. From 17 to *ca.* 13 ka cal BP, as shown in Figure 2, the dominant cold and dry winter monsoon transported a large quantity of dust from the loess source area, depositing a layer 5 m thick at the base of the profile at an average rate of 0.16 cm yr^{-1}.

From *ca.* 13–10.9 ka cal BP, solar radiation increased and the summer monsoon strengthened, allowing soil development. Two peaks of magnetic susceptibility and TOCC with more negative $\delta^{13}C$ occur. This episode lasted *ca.* 2 ka.

Subsequently, for the next *ca.* 700 yr (10.9–10.2 ka cal BP), an abrupt climatic reversal brought on conditions that led to the deposition of 1.25 m of loess, which interrupted the development of the paleosol sequence. During this period, the dominant summer monsoon rapidly weakened and the winter monsoon strengthened. Loess deposition rate reached a mean value of 0.23 cm yr^{-1}, which is the maximum for the entire Baxie profile. The SUS, $\delta^{13}C$ and TOCC curves show an obvious trough, reflecting a shift to a desert-steppe landscape typical of a cold, dry climate. The beginning and termination of this event appear to be later by about 1 ka than the time of the Younger Dryas event in the North Atlantic region (12.1–11.3 ka cal BP) (Stuiver *et al.* 1991).

From 10–6 ka cal BP, a black-loam paleosol complex, 3 m thick, developed at Baxie. The SUS index and TOCC reached their highest values, and $\delta^{13}C$ values were more negative, reflecting the strengthening of the summer monsoon and increased precipitation. By extrapolation from the ^{14}C age of 6670 cal BP, and using the sedimentation rate, the age of the top of the paleosol complex (4.90 m depth) is calculated as 6170 cal BP. This record is consistent with the atmospheric circulation model in northern hemisphere tropic and sub-tropic regions reported by Kutzbach and Street-Perrott (1985); *i.e.*, from 15 ka BP onward, monsoon circulation strengthened and precipitation increased in the northern hemisphere tropics, culminating *ca.* 9–6 ka BP. The July temperature and precipitation/evaporation values were also higher than today. This kind of record can be found in other profiles on the Loess Plateau (Zhou & An 1991), and shows a strong correlation with the amplitude of the seasonal solar radiation cycle. An *et al.* (1990) pointed out that the higher amplitude of this cycle is one of the important factors triggering the strengthened east Asian monsoon circulation. Different thermal capacities of ocean and land vary their responses to

the seasonal radiation cycle. Thus, the normal monsoon circulation is strengthened (*i.e.*, both summer and winter monsoons are strengthened).

ACKNOWLEDGMENTS

REFERENCES

Aitken, M. J. 1985 *Thermoluminescence Dating*. London, Academic Press: 66–67.

An, Z., Liu, T., Lu, Y., Porter, S. C., Kukla, G., Wu, X. and Hua, Y. 1991 The long-term paleomonsoon variation recorded by loess-paleosol sequence in central China. *Quaternary International* 7, in press.

An, Z. S., Xiao, J., Zhang, J. Z., Xie, J., Zheng, H. P. and Zhao, H. 1990 Monsoon and climatic history during the last 130,000 years in the Loess Plateau, China. In *Loess Quaternary Geology Global Change*. Beijing, Science Press: 108–114.

Fleming, S. J. 1979 *Thermoluminescence Techniques in Archaeology*. Oxford, Clarendon Press: 30–33.

Head, M. J., Zhou, W. J. and Zhou, M. F. 1989 Evaluation of ^{14}C ages of organic fractions of paleosols from loess-paleosol sequences near Xian, China. *In* Long, A. and Kra, R. S., eds., Proceedings of the 13th International ^{14}C Conference. *Radiocarbon* 31(3): 680–696.

Heller, F. and Liu, T. S. 1986 Paleoclimatic and sedimentary history from magnetic susceptibility of loess in China. *Geophysical Research Letters* 13: 1169–1172.

Kukla, G. and An, Z. S. 1989 Loess stratigraphy in central China. *Palaeogeography, Palaeoclimatology, Palaeoecology* 72: 203–225.

Kutzbach, J. and Street-Perrott, F. 1985 Milankovich forcing of fluctuations in the level of tropical lakes from 18 K to present. *Nature* 317: 130–134.

Liu, T. S., ed. 1985 *Loess and the Environment*. Beijing, China, Ocean Press: 251.

Maher, B. A. and Thompson, R. 1992 Paleoclimatic significance of the minimal magnetic record of the Chinese loess and paleosols. *Quaternary Research* 37: 155–170.

Prescott, J. R. and Stephan, L. G. 1982 Contribution of cosmic rays to the environmental dose for thermoluminescence dating latitude altitude and depth dependence. *PACT* 6: 15–17.

Qiao, Y. 1985 ^{14}C Dating of loess. *In* Liu, T. S., ed., *Loess and the Environment*. Beijing, China, Ocean Press: 48–53.

Readhead, M. L. 1982 Extending thermoluminescence dating to geological sediments. *In* Ambrose, W. and Duerden, P., eds., *Archaeometry: An Australian Perspective*. Canberra, ANU Press: 276–281.

Singhvi, A. K., Sharma, Y. P. and Agrawal, D. P. 1982 Thermoluminescence dating of sand dunes in Rajasthan India. *Nature* 295: 313–315.

Slota, P. J., Jr., Jull, A. J. T., Linick, T. W. and Toolin, L. J. 1987 Preparation of small samples for ^{14}C accelerator targets by catalytic reduction of CO. *Radiocarbon* 29(2): 303–306.

Steinberg, C. and Muenster, U. 1985 Geochemistry and ecological role of humic substances in lake water. *In* Aiken, G. R., McKnight, D. M., Wershaw, R. L. and McCarthy, P., eds., *Humic Substances in Soil Sediment and Water Geochemistry Isolation and Characterisation*. New York, John Wiley & Sons: 105–146.

Stevenson, F. J. 1986 *Cycles of Soil: Carbon Nitrogen Phosphorus. Sulphur Micronutrients*. New York, John Wiley & Sons: 380.

Stuiver, M., Braziunas, T. F., Becker, B. and Kromer, B. 1991 Climatic solar oceanic and geomagnetic influences on Late-Glacial and Holocene atmospheric ^{14}C/^{12}C change. *Quaternary Research* 35: 1–24.

Stuiver, M. and Pearson, G. W. 1986 High-precision calibration of the radiocarbon time scale, AD 1950–500 BC. *In* Stuiver, M. and Kra, R. S., eds., Proceedings of the 12th International ^{14}C Conference. *Radiocarbon* 28(2B): 805–838.

Wintle, A. G. and Huntley, D. J. 1982 Thermoluminescence dating of sediments. *Quaternary Science Reviews* 1: 31–35.

Zhang, L. 1989 Landslide history and late Cenozoic environmental factors in the Sa Le Shan area Dongxian County Gansu Province China. *In* Proceedings of the International Conference on Loess Geomorphic Processes and Hazards. *Journal of Lanzhou University*: 81–93.

Zheng, H. 1985 Distribution of Holocene loess. *In* Liu, T. S., ed., *Loess and the Environment*. Beijing, China, Ocean Press: 53–59.

Zhou, W. J. and An, Z. S. 1991 ^{14}C chronology of the Loess Plateau in China. *Proceedings of INQUA Conference*. Beijing, in press.

Zhou, W. J., Zhou, M. F. and Head, J. 1990 ^{14}C chronology of Beizhuang Cun sedimentation sequence since 30,000 years BP. *Chinese Science Bulletin* 35(7): 567–572.